Electric Toroidal Quadrupoles in the Spin-Orbit-Coupled Metal $Cd_2Re_2O_7$

Satoru Hayami,[1] Yuki Yanagi,[2] Hiroaki Kusunose,[2] and Yukitoshi Motome[3]
[1]*Faculty of Science, Hokkaido University, Sapporo 060-0810, Japan*
[2]*Department of Physics, Meiji University, Kawasaki 214-8571, Japan*
[3]*Department of Applied Physics, University of Tokyo, Tokyo 113-8656, Japan*

(Received 26 November 2018; published 11 April 2019)

We report our theoretical results on the order parameters for the pyrochlore metal $Cd_2Re_2O_7$, which undergoes enigmatic phase transitions with inversion symmetry breaking. By carefully examining active electronic degrees of freedom based on the lattice symmetry, we propose that two parity-breaking phases at ambient pressure are described by unconventional multipoles, *electric toroidal quadrupoles* (ETQs) with different components, x^2-y^2 and $3z^2-r^2$, in the pyrochlore tetrahedral unit. We elucidate that the ETQs are activated by bond or spin-current order on Re—Re bonds. Our ETQ scenario provides a key to reconciling the experimental contradictions, by measuring ETQ specific phenomena, such as peculiar spin splittings in the electronic band structure, magnetocurrent effect, and nonreciprocal transport under a magnetic field.

DOI: 10.1103/PhysRevLett.122.147602

Introduction.—The spin-orbit coupling in crystals with a lack of spatial inversion symmetry, dubbed the antisymmetric spin-orbit coupling (ASOC), has attracted great interest in condensed matter physics. It is a source of intriguing phenomena, such as Dirac electrons at the surface of topological insulators [1,2], the spin Hall effect [3,4], multiferroics [5–7], and noncentrosymmetric superconductivity [8]. Such ASOC-related physics has been found in a variety of materials irrespective of insulators (semiconductors) [9–12] and metals [13–16] in p-, d-, and f-electron systems. Thus, the ASOC is highly expected to bring a new route toward applications to next-generation electronics and spintronics devices [17,18].

Of special interest is to control the ASOC by spontaneous inversion symmetry breaking in electronic degrees of freedom (d.o.f.). Such parity breaking can generate odd-parity multipoles, e.g., magnetic quadrupoles (MQs) and electric octupoles (EOs) [19–26]. They provide a fertile ground for exploring new types of multipole orders [27–34] and unconventional superconductivities [35–38]. The pyrochlore oxide $Cd_2Re_2O_7$ is a prototype compound for such spontaneous inversion symmetry breaking in the presence of the strong spin-orbit coupling [30,39]. The system exhibits a surprisingly complex phase diagram while changing temperature and pressure, including a collection of spontaneously parity-breaking phases [40–43]. In addition, among many pyrochlores, it is the only superconductor thus far [44–48]. The superconducting state also shows unconventional behavior under pressure, presumably due to the spontaneous parity breaking [35,36,40].

At ambient pressure, $Cd_2Re_2O_7$ undergoes a continuous structural phase transition at $T_{s1}\sim 200$ K, from the centrosymmetric cubic phase with $Fd\bar{3}m$ symmetry (phase I) to the noncentrosymmetric tetragonal one (phase II). As the tetragonal lattice distortion is very small, evaluated at most 0.05% [49], the transition is considered to be of electronic origin. However, the space-group symmetry in phase II is still controversial; it was identified as $I\bar{4}m2$ by the single-crystal x-ray diffraction (XRD) [49,50], powder neutron diffraction [51], convergent beam electron diffraction (CBED) [52], Raman spectroscopy [53], nonlinear optics [54], and polarizing microscope image (PMI) [55], while the recent nonlinear optical measurements indicated further symmetry reduction to $I\bar{4}$, $I\bar{4}m'2'$, or $I\bar{4}m'$ [34,56,57]. Moreover, another structural transition to phase III occurring at $T_{s2}\sim 120$ K is also controversial; the single-crystal XRD [50,58], CBED [52], and PMI [55] measurements indicated a first-order transition to $I4_122$, while the nonlinear optical measurements indicated the absence of a phase transition [54]. Toward comprehensive understanding of the rich physics by spontaneous parity breaking and emergent ASOC in this compound, it is desirable to resolve the experimental contradictions and clarify the origin of the enigmatic phase transitions.

In this Letter, we investigate which types of electronic instability can occur in the spin-orbit-coupled metal $Cd_2Re_2O_7$ at ambient pressure from the viewpoint of odd-parity multipoles. Relying on the lattice symmetry by the single-crystal XRD [50], we here concentrate on odd-parity multipoles with E_u symmetry [59]. We find that the primary order parameters in phases II and III are described by electric toroidal quadrupoles (ETQs) with specific bond modulations in the tetrahedral unit of the pyrochlore structure with different components of x^2-y^2 and $3z^2-r^2$, respectively. We note that the ETQs were pointed out as secondary order parameters based on the nonlinear optical measurements [34]. By performing a microscopic analysis for a generic tight-binding model

on the pyrochlore structure, we show that spontaneous bond or spin-current ordering on Re—Re bonds is essential to induce the ETQs. We also present how to detect the ETQs in experiments by elucidating ETQ-driven phenomena, such as the spin-split Fermi surface, the magnetocurrent (MC) effect, and nonreciprocal transport (NRT) in an applied magnetic field.

Symmetry argument.—First, we discuss the candidates of order parameters for phases II and III in $Cd_2Re_2O_7$ from a symmetry point of view. In order to describe the electronic d.o.f. in crystals, we introduce four types of multipoles: conventional electric and magnetic multipoles (polar and axial tensors, respectively), and unconventional electric toroidal (ET) and magnetic toroidal (MT) multipoles (axial and polar tensors) (see the Supplemental Material [60]). Any types of symmetry breaking can be described by the multipoles [63]. In particular, the parity-breaking order parameters are described by odd-rank electric (MT) multipoles and even-rank ET (magnetic) multipoles in the presence (absence) of time-reversal symmetry.

We classify the relevant odd-parity multipoles in Table I with respect to the irreducible representation of the cubic O_h group in phase I. We also present the space-subgroup symmetry for each odd-parity multipole within the symmetries supported by the XRD results [50]. Since the XRD measurements [50] indicate that the space-group symmetries in phases II and III are $I\bar{4}m2$ and $I4_122$, respectively, and since $Cd_2Re_2O_7$ is most likely nonmagnetic (time-reversal even) [64], we deduce that the primary order parameters are the ETQs with different components: G_v for phase II and G_u for phase III, where the subscripts v and u represent different quadrupole components of x^2-y^2 and $3z^2-r^2$, respectively [34,65]. In the following, we examine what types of electronic instability can induce the two ETQs from a microscopic point of view.

TABLE I. Classification of odd-parity multipoles with respect to the irreducible representation (irrep) of the point group O_h. The superscripts "+" and "−" denote time-reversal even and odd, respectively. The odd-parity multipoles are shown with their multipole type, rank, notation, and space-group symmetry where details are shown in the Supplemental Material [60]. ETM, MM, EO, MTO, ETQ, MQ, ED, and MTD represent electric toroidal monopole, magnetic monopole, electric octupole, magnetic toroidal octupole, electric toroidal quadrupole, magnetic quadrupole, electric dipole, and magnetic toroidal dipole, respectively. ν_{BO} and ν_{SCO} represent the number of modes in each irrep for the bond and spin-current ordered states, respectively.

Irrep	Multipole	Rank	Notation	Symmetry	ν_{BO}	ν_{SCO}
$A_{1u}^{+}; A_{1u}^{-}$	ETM; MM	0	$G_0; M_0$	$F4_132\,(O)$	0; 0	1; 1
$A_{2u}^{+}; A_{2u}^{-}$	EO; MTO	3	$Q_{xyz}; T_{xyz}$	$F\bar{4}3m\ (T_d)$	1; 0	1; 0
$E_u^{+}; E_u^{-}$	ETQ; MQ	2	$G_u; M_u$	$I4_122\ (D_4)$	1; 0	2; 1
			$G_v; M_v$	$I\bar{4}m2\ (D_{2d})$		
$T_{1u}^{+}; T_{1u}^{-}$	ED; MTD	1	$Q_z; T_z$	$I4_1\ (C_4)$	1; 1	2; 2
			$Q_x; T_x$			
			$Q_y; T_y$			
$T_{2u}^{+}; T_{2u}^{-}$	ETQ; MQ	2	$G_{xy}; M_{xy}$	$I\bar{4}\ (S_4)$	0; 1	2; 3
			$G_{yz}; M_{yz}$			
			$G_{zx}; M_{zx}$			

Electric toroidal quadrupoles.—Next, in order to clarify how the ETQs are activated in the electronic d.o.f., we perform a microscopic analysis based on the tight-binding model. While $Cd_2Re_2O_7$ is a multiorbital system with relevant t_{2g} orbitals for $5d$ electrons [66,67], we consider an effective single-orbital model and concentrate on the geometrical effect from the pyrochlore structure composed of the tetrahedron unit. An extension to multiorbital models is straightforward by supplementing additional symmetry operations for atomic orbitals at each site. The Hamiltonian for the effective tight-binding model is given as

$$\mathcal{H}=\sum_{\boldsymbol{k}\alpha\beta\gamma}\sum_{ij\sigma\sigma'}c^{\dagger}_{\boldsymbol{k}i\sigma}[\{f^{S}_{\alpha\beta\gamma}(\boldsymbol{k})+f^{A}_{\alpha\beta\gamma}(\boldsymbol{k})\}\rho_\alpha\tau_\beta\sigma_\gamma]^{\sigma\sigma'}_{ij}c_{\boldsymbol{k}j\sigma'}, \quad (1)$$

where $c^{\dagger}_{\boldsymbol{k}i\sigma}$ ($c_{\boldsymbol{k}i\sigma}$) is the creation (annihilation) operator for wave vector $\boldsymbol{k}$, sublattice $i=A$–D, and spin σ. Here, the positions of the four sublattice sites within the tetrahedral unit cell are defined by $\boldsymbol{r}_A=(0,0,0)$, $\boldsymbol{r}_B=(a/4,a/4,0)$, $\boldsymbol{r}_C=(a/4,0,a/4)$, and $\boldsymbol{r}_D=(0,a/4,a/4)$ [see Fig. 1(a); we set $a=1$ as the unit of length]. The four sublattice d.o.f. is described by the product of two Pauli matrices ρ_α and τ_β for $\alpha,\beta=0,x,y,z$; ρ_α spans A–B and C–D, and τ_β spans (AB)–(CD). σ_γ describes 2×2 spin space for $\gamma=0,x,y,z$. $f^{S}_{\alpha\beta\gamma}(\boldsymbol{k})$ and $f^{A}_{\alpha\beta\gamma}(\boldsymbol{k})$ are symmetric and asymmetric form factors with

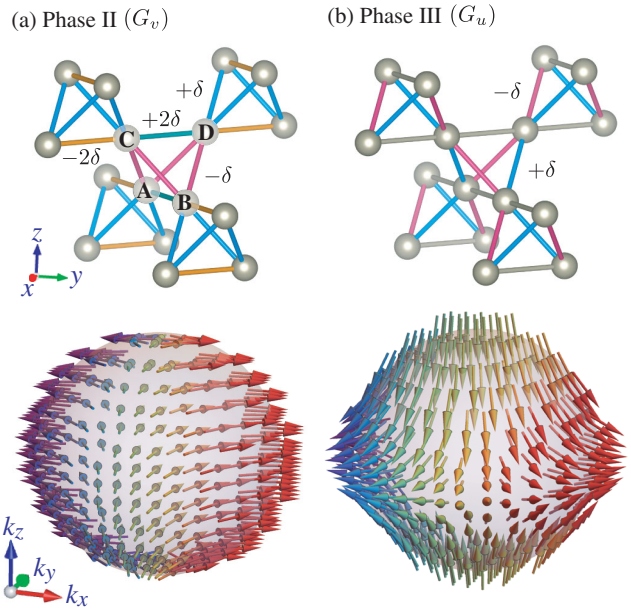

FIG. 1. Schematic pictures of the bond modulations caused by the electric toroidal quadrupoles (ETQs): (a) G_v for phase II and (b) G_u for phase III. Schematic spin polarizations on one of the Fermi surfaces split by the ETQ orderings are shown in the bottom figures. We assume the spherical Fermi surfaces for simplicity.

respect to $\boldsymbol{k}$, which are related with even- and odd-parity multipoles, respectively. Note that Eq. (1) can describe all possibilities of symmetry-breaking mean fields as well as the (spin-dependent) electron hoppings [60].

As the Hamiltonian in Eq. (1) is an 8×8 matrix denoted by the direct product of three Pauli matrices, $\rho_\alpha \tau_\beta \sigma_\gamma$, the total number of independent electronic d.o.f. is $8 \times 8 \times 2 = 128$, where the factor 2 comes from symmetric or antisymmetric nature with respect to $\boldsymbol{k}$, i.e., $f^S_{\alpha\beta\gamma}$ and $f^A_{\alpha\beta\gamma}$. The 128 electronic d.o.f. are categorized into the 16 on-site potential types, 96 nearest-neighbor (NN) bond types, and 16 third-neighbor bond types [60]. Among them, we neglect the 16 on-site potential-type order parameters, as they do not break spatial inversion symmetry. We also exclude the 16 third-neighbor bond types because their amplitudes are usually smaller than the NN ones. For the remaining 96 NN bond types, we try to elucidate how they activate the ETQs.

Let us first consider the ETQs without spin d.o.f. In the spinless subspace, the number of electronic d.o.f. about the NN bond type is reduced to 24. They are decomposed into the irreducible representations $(A^+_{1g} \oplus E^+_g \oplus T^+_{2g}) \oplus (A^+_{2u} \oplus E^+_u \oplus T^+_{1u}) \oplus (T^-_{1g} \oplus T^-_{2g}) \oplus (T^-_{1u} \oplus T^-_{2u})$, where the superscripts "+" and "−" represent time-reversal even and odd, respectively. From the decomposition, we find that six types of NN bond modulations can induce odd-parity multipoles of time-reversal even: EO Q_{xyz}, two ETQs (G_u, G_v), and three electric dipoles (Q_x, Q_y, Q_z) (see Table I). This indicates that the ETQs G_u and G_v, which we identified as the order parameters in $Cd_2Re_2O_7$, can be activated through spontaneous bond orderings (BOs). By taking an appropriate linear combination of $f^A_{\alpha\beta\gamma}(\boldsymbol{k})\rho_\alpha\tau_\beta\sigma_\gamma$ [60], we obtain the microscopic expressions for the ETQs as

$$G_u = \delta[-s_x c_z \rho_z \tau_y + s_y c_z \rho_y \tau_x + s_z (c_y \rho_x \tau_y - c_x \tau_y)], \quad (2)$$

$$G_v = \delta[s_x (2c_y \rho_y \tau_z - c_z \rho_z \tau_y) + s_y (2c_x \rho_y - c_z \rho_y \tau_x) - s_z (c_x \tau_y + c_y \rho_x \tau_y)], \quad (3)$$

where $s_\mu = \sin(k_\mu/4)$ and $c_\mu = \cos(k_\mu/4)$ $(\mu = x, y, z)$, and δ represents the degree of bond modulations, which corresponds to the order parameter amplitude. The bond modulations are schematically shown in Fig. 1: (a) for G_v in phase II [Eq. (3)] and (b) for G_u in phase III [Eq. (2)]. Note that each atomic site is no longer the inversion center in these states, reflecting the odd parity of G_v and G_u. We list the number of modes (independent order parameters) in the BO states in Table I.

We next discuss the ETQs with spin d.o.f. As spins are time-reversal odd, the odd-parity multipoles of time-reversal even are constructed by combining the Pauli matrix σ_γ and the above spinless odd-parity multipoles with time-reversal odd, i.e., the MT dipoles (T_x, T_y, T_z) belonging to T^-_{1u} and MQs (M_{yz}, M_{zx}, M_{xy}) belonging to T^-_{2u}, as shown in Table I.

By regarding σ_γ as an axial magnetic dipole belonging to T^-_{2g}, the odd-parity multipoles of time-reversal even in the spinful case are obtained in the irreducible representations of $(T^-_{1u} \oplus T^-_{2u}) \otimes T^-_{2g} \to A^+_{1u} \oplus A^+_{2u} \oplus 2E^+_u \oplus 2T^+_{1u} \oplus 2T^+_{2u}$. Consequently, we find four types of active ETQs, $2E^+_u$, whose microscopic expressions are represented by

$$G^{\sigma(1)}_u = 2\sigma_z T_z - \sigma_x T_x - \sigma_y T_y, \quad (4)$$

$$G^{\sigma(2)}_u = \sigma_x M_{yz} - \sigma_y M_{zx}, \quad (5)$$

$$G^{\sigma(1)}_v = \sigma_x T_x - \sigma_y T_y, \quad (6)$$

$$G^{\sigma(2)}_v = 2\sigma_z M_{xy} - \sigma_x M_{yz} - \sigma_y M_{zx}, \quad (7)$$

where the superscript σ denotes that the ETQs have spin dependence; (T_x, T_y, T_z) and (M_{yz}, M_{zx}, M_{xy}) are also represented by an appropriate linear combination of $f^A_{\alpha\beta\gamma}(\boldsymbol{k})\rho_\alpha\tau_\beta$ as Eqs. (2) and (3) (see the Supplemental Material [60]).

The ETQs in Eqs. (4)–(7) are also activated through a bond-order-type instability like those in the spinless case in Eqs. (2) and (3). However, they originate from asymmetric modulations of time-reversal-odd imaginary hoppings in the spin-dependent form, which can be regarded as spin-current orders (SCOs) [60]. In Fig. 2, we exemplify the MT dipole T_z and MQ M_{xy}, in which the arrows on each bond represent the imaginary hoppings [68]. This type of SCO has been studied in the context of topological Mott insulators [69,70]. We list the number of modes in the SCO state in Table I.

Secondary order parameters.—As direct observation of ETQs is rather difficult, we discuss what types of multipoles are additionally induced as the secondary order parameters under the ETQ orders from symmetry arguments [65]. In phase II with $I\bar{4}m2$ (D_{2d}) symmetry, since A_{2u} reduces to symmetric representations A_1, the odd-parity EO Q_{xyz} is induced as a secondary order parameter.

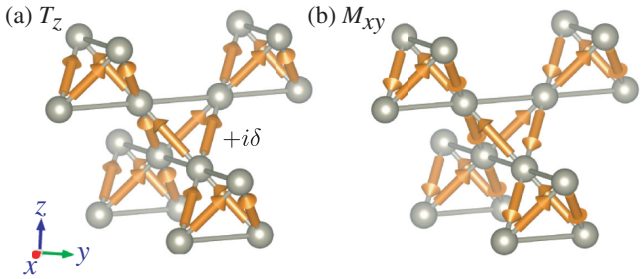

FIG. 2. Schematic pictures of the bond modulations in the presence of (a) the magnetic toroidal dipole T_z and (b) the magnetic quadrupole M_{xy}. Their microscopic expressions are shown in the Supplemental Material [60]. The arrows on the bonds represent the imaginary hoppings; the tail-to-head directions denote the positive imaginary hoppings.

Meanwhile, in phase III, the odd-parity ET monopole G_0 (time-reversal-even pseudoscalar) is induced as a secondary order parameter, since A_{1u} reduces to symmetric representations under the $I4_122$ (D_4) symmetry. Furthermore, in both phases II and III, since E_g reduces to symmetric representations $A_1 \oplus B_1$, the even-parity electric quadrupole Q_u is induced as a secondary order parameter. The observation of these secondary order parameters can be indirect evidence of the ETQ orders. For instance, ultrasound and magnetic torque measurements may detect the electric quadrupole [71–74].

ETQ-driven phenomena.—For further identification of the ETQs, we discuss physical phenomena driven by the ETQ orderings [60]. As the ETQs break spatial inversion symmetry, the band structures in both phases II and III exhibit spin splitting as the Rashba metals [30,56]. The origin of such spin splitting is the ASOC induced by the ETQ orderings. The functional form of the ASOC is derived by considering the active odd-parity multipoles belonging to symmetric representations in their space groups [65,75]: G_v and Q_{xyz} in phase II, and G_u and G_0 in phase III. In particular, the odd-parity multipoles with rank 0–2 lead to the ASOC in the first order of $\boldsymbol{k}$ [65]. The resultant functional forms of the ASOC for phases II and III are given by

$$\mathcal{H}^{\mathrm{II}}_{\mathrm{ASOC}} = c_1(k_x\sigma_x - k_y\sigma_y) + O(k^3), \tag{8}$$

$$\mathcal{H}^{\mathrm{III}}_{\mathrm{ASOC}} = c_1(k_x\sigma_x + k_y\sigma_y) + c_2k_z\sigma_z + O(k^3), \tag{9}$$

respectively, where c_1 and c_2 are appropriate constants proportional to the order parameter amplitude δ. The spin polarizations described by Eqs. (8) and (9) are schematically shown on the spherical Fermi surfaces in the lower pictures of Figs. 1(a) and 1(b), respectively. Although $Cd_2Re_2O_7$ has the multiple and complicated Fermi surfaces [76], the real spin polarizations are obtained by projecting the pictures in Figs. 1(a) and 1(b) onto the actual Fermi surface. Note that such spin splitting in the band structure occurs even for the spinless ETQs in Eqs. (2) and (3) in the presence of the spin-orbit coupling.

In addition, the ETQs give rise to intriguing responses to external stimuli. One is the MC effect, in which a uniform magnetization M_i is induced by an electric current J_j ($i, j = x, y, z$) as [65,75]

$$M_i = \alpha_{ij}J_j, \tag{10}$$

where the MC tensor α_{ij} is the rank-2 axial tensor of time-reversal even. The form of α_{ij} is related to active odd-parity multipoles with rank 0–2 ($G_0 \oplus Q_{1m} \oplus G_{2m}$) [65]; the rank-0, -1, and -2 multipoles have the isotropic, antisymmetric, and symmetric traceless components, respectively. Thus, α_{ij} in phase II becomes symmetric and traceless corresponding to G_v: $\alpha_{xx} = -\alpha_{yy} \propto G_v$. Meanwhile, α_{ij} in phase III has two nonzero symmetric components reflecting G_0 and G_u: $\alpha_{xx} = \alpha_{yy} \propto G_0 - G_u$ and $\alpha_{zz} \propto G_0 + 2G_u$. The results are summarized in Table II.

TABLE II. Nonzero components of the magnetocurrent (MC) tensor α_{ij} and nonreciprocal transport (NRT) tensor σ_{ijkl} expected under the electric toroidal quadrupole (ETQ) orderings. EO, EQ, and ETM represent electric octupole, electric quadrupole, and electric toroidal monopole, respectively. The results for the NRT are shown for both primary (op1) and secondary (op2) order parameters. See the text for details.

Phase II	op1: G_v (ETQ), op2: Q_{xyz} (EO), Q_u (EQ)
MC	$\alpha_{xx} = -\alpha_{yy}$
NRT	$\sigma_{xxxx} = -\sigma_{yyyy}$, $\sigma_{xxyy} = -\sigma_{yyxx}$, $\sigma_{xyyx} = -\sigma_{yxxy}$, $\sigma_{xxzz} = -\sigma_{yyzz}$, $\sigma_{xzzx} = -\sigma_{yzzy}$, $\sigma_{zzxx} = -\sigma_{zzyy}$, $\sigma_{zxxz} = -\sigma_{zyyz}$
Phase III	**op1: G_u (ETQ), op2: G_0 (ETM), Q_u (EQ)**
MC	$\alpha_{xx} = \alpha_{yy}$, α_{zz}
NRT	$\sigma_{xxxx} = \sigma_{yyyy}$, $\sigma_{xxyy} = \sigma_{yyxx}$, $\sigma_{xyyx} = \sigma_{yxxy}$, $\sigma_{xxzz} = \sigma_{yyzz}$, $\sigma_{xzzx} = \sigma_{yzzy}$, $\sigma_{zzxx} = \sigma_{zzyy}$, $\sigma_{zxxz} = \sigma_{zyyz}$, σ_{zzzz}

Another interesting response is the NRT. As a nonreciprocal current is proportional to the second order of an electric field, the NRT needs the breaking of time-reversal symmetry by an external magnetic field as

$$J_i = \sigma_{ijkl}E_jE_kH_l, \tag{11}$$

where the NRT tensor σ_{ijkl} is the rank-4 axial tensor; E_j and H_l are electric and magnetic fields, respectively. From symmetry arguments, the form of the NRT tensor is related to the multipoles with rank 0–4 ($2G_0 \oplus 3Q_{1m} \oplus 4G_{2m} \oplus 2Q_{3m} \oplus G_{4m}$) [65]. Consequently, σ_{ijkl} has independent seven (eight) components in phase II (III), as shown in Table II. We note that higher-order ET hexadecapoles also become active: G_{4v} in phase II, and G_4 and G_{4u} in phase III.

It is also interesting to point out that a lattice distortion is induced by an electric current in an applied magnetic field as $\zeta_{ij} = d_{ijkl}J_kH_l$, where d_{ijkl} represents a strain tensor [65,75]. This is easily understood by noting that E_jE_k in Eq. (11) and ζ_{ij} show the same transformation under the space-time inversion. Thus, the tensor d_{ijkl} has similar nonzero components to σ_{ijkl} in Eq. (11).

Conclusion.—We theoretically showed that the odd-parity electric toroidal quadrupoles with different components of $x^2 - y^2$ and $3z^2 - r^2$ are the candidates of the primary order parameters in phases II and III, respectively, in the spin-orbit-coupled metal $Cd_2Re_2O_7$. We clarified that electronic instabilities toward spontaneous bond or spin-current ordering on Re—Re bonds induce the electric toroidal quadrupole orders. We also discussed how to identify the electric toroidal quadrupoles by exemplifying their characteristic phenomena, such as spin-split Fermi surfaces, magnetocurrent effect, and nonreciprocal transport in an applied magnetic field. Our electric toroidal quadrupole scenario will give an insight into the origin of

the enigmatic phase transitions in $Cd_2Re_2O_7$. Furthermore, our microscopic classifications of multipoles are generic to not only other pyrochlore systems [77] but also spontaneously parity-breaking systems, which are useful when the order parameter is complicated and unknown.

The authors thank Z. Hiroi, M. Takigawa, J. Yamaura, S. Uji, D. Hirai, and H. Hirose for the fruitful discussions on experimental information in $Cd_2Re_2O_7$. This research was supported by JSPS KAKENHI Grants No. JP15H05885, No. JP18H04296 (J-Physics), and No. JP18K13488.

[1] M. Z. Hasan and C. L. Kane, Rev. Mod. Phys. **82**, 3045 (2010).
[2] X.-L. Qi and S.-C. Zhang, Rev. Mod. Phys. **83**, 1057 (2011).
[3] J. E. Hirsch, Phys. Rev. Lett. **83**, 1834 (1999).
[4] J. Sinova, D. Culcer, Q. Niu, N. A. Sinitsyn, T. Jungwirth, and A. H. MacDonald, Phys. Rev. Lett. **92**, 126603 (2004).
[5] M. Fiebig, J. Phys. D **38**, R123 (2005).
[6] S.-W. Cheong and M. Mostovoy, Nat. Mater. **6**, 13 (2007).
[7] D. Khomskii, Physics **2**, 20 (2009).
[8] *Non-centrosymmetric Superconductors: Introduction and Overview*, edited by E. Bauer and M. Sigrist, Lecture Notes in Physics Vol. 847 (Springer, New York, 2012).
[9] M. S. Dresselhaus, G. Dresselhaus, and A. Jorio, *Group Theory: Application to the Physics of Condensed Matter* (Springer-Verlag, Berlin, 2008).
[10] K. Ishizaka, M. Bahramy, H. Murakawa, M. Sakano, T. Shimojima, T. Sonobe, K. Koizumi, S. Shin, H. Miyahara, A. Kimura *et al.*, Nat. Mater. **10**, 521 (2011).
[11] T. Furukawa, Y. Shimokawa, K. Kobayashi, and T. Itou, Nat. Commun. **8**, 954 (2017).
[12] T. Ideue, K. Hamamoto, S. Koshikawa, M. Ezawa, S. Shimizu, Y. Kaneko, Y. Tokura, N. Nagaosa, and Y. Iwasa, Nat. Phys. **13**, 578 (2017).
[13] E. Bauer, G. Hilscher, H. Michor, C. Paul, E. W. Scheidt, A. Gribanov, Y. Seropegin, H. Noël, M. Sigrist, and P. Rogl, Phys. Rev. Lett. **92**, 027003 (2004).
[14] A. Ashrafi and D. L. Maslov, Phys. Rev. Lett. **109**, 227201 (2012).
[15] W. Witczak-Krempa, G. Chen, Y. B. Kim, and L. Balents, Annu. Rev. Condens. Matter Phys. **5**, 57 (2014).
[16] H. Saito, K. Uenishi, N. Miura, C. Tabata, H. Hidaka, T. Yanagisawa, and H. Amitsuka, J. Phys. Soc. Jpn. **87**, 033702 (2018).
[17] I. Žutić, J. Fabian, and S. Das Sarma, Rev. Mod. Phys. **76**, 323 (2004).
[18] V. Baltz, A. Manchon, M. Tsoi, T. Moriyama, T. Ono, and Y. Tserkovnyak, Rev. Mod. Phys. **90**, 015005 (2018).
[19] Y. Yanase, J. Phys. Soc. Jpn. **83**, 014703 (2014).
[20] T. Hitomi and Y. Yanase, J. Phys. Soc. Jpn. **83**, 114704 (2014).
[21] T. Hitomi and Y. Yanase, J. Phys. Soc. Jpn. **85**, 124702 (2016).
[22] K. Kimura, P. Babkevich, M. Sera, M. Toyoda, K. Yamauchi, G. Tucker, J. Martius, T. Fennell, P. Manuel, D. Khalyavin *et al.*, Nat. Commun. **7**, 13039 (2016).
[23] Y. Kato, K. Kimura, A. Miyake, M. Tokunaga, A. Matsuo, K. Kindo, M. Akaki, M. Hagiwara, M. Sera, T. Kimura *et al.*, Phys. Rev. Lett. **118**, 107601 (2017).
[24] N. D. Khanh, N. Abe, S. Kimura, Y. Tokunaga, and T. Arima, Phys. Rev. B **96**, 094434 (2017).
[25] Y. Yanagi, S. Hayami, and H. Kusunose, Phys. Rev. B **97**, 020404 (2018).
[26] S. Hayami, H. Kusunose, and Y. Motome, Phys. Rev. B **97**, 024414 (2018).
[27] E. Fradkin, S. A. Kivelson, M. J. Lawler, J. P. Eisenstein, and A. P. Mackenzie, Annu. Rev. Condens. Matter Phys. **1**, 153 (2010).
[28] S. Hayami, H. Kusunose, and Y. Motome, Phys. Rev. B **90**, 024432 (2014).
[29] S. Hayami, H. Kusunose, and Y. Motome, Phys. Rev. B **90**, 081115 (2014).
[30] L. Fu, Phys. Rev. Lett. **115**, 026401 (2015).
[31] M. R. Norman, Phys. Rev. B **92**, 075113 (2015).
[32] S. Hayami, H. Kusunose, and Y. Motome, J. Phys. Condens. Matter **28**, 395601 (2016).
[33] H. Watanabe and Y. Yanase, Phys. Rev. B **96**, 064432 (2017).
[34] S. Di Matteo and M. R. Norman, Phys. Rev. B **96**, 115156 (2017).
[35] V. Kozii and L. Fu, Phys. Rev. Lett. **115**, 207002 (2015).
[36] Y. Wang, G. Y. Cho, T. L. Hughes, and E. Fradkin, Phys. Rev. B **93**, 134512 (2016).
[37] F. Wu and I. Martin, Phys. Rev. B **96**, 144504 (2017).
[38] S. Sumita, T. Nomoto, and Y. Yanase, Phys. Rev. Lett. **119**, 027001 (2017).
[39] Z. Hiroi, J.-i. Yamaura, T. C. Kobayashi, Y. Matsubayashi, and D. Hirai, J. Phys. Soc. Jpn. **87**, 024702 (2018).
[40] T. C. Kobayashi, Y. Irie, J.-i. Yamaura, Z. Hiroi, and K. Murata, J. Phys. Soc. Jpn. **80**, 023715 (2011).
[41] N. Barišić, L. Forró, D. Mandrus, R. Jin, J. He, and P. Fazekas, Phys. Rev. B **67**, 245112 (2003).
[42] J.-i. Yamaura, K. Takeda, Y. Ikeda, N. Hirao, Y. Ohishi, T. C. Kobayashi, and Z. Hiroi, Phys. Rev. B **95**, 020102 (2017).
[43] I. A. Sergienko and S. H. Curnoe, J. Phys. Soc. Jpn. **72**, 1607 (2003).
[44] M. Hanawa, Y. Muraoka, T. Tayama, T. Sakakibara, J. Yamaura, and Z. Hiroi, Phys. Rev. Lett. **87**, 187001 (2001).
[45] H. Sakai, K. Yoshimura, H. Ohno, H. Kato, S. Kambe, R. E. Walstedt, T. D. Matsuda, Y. Haga, and Y. Onuki, J. Phys. Condens. Matter **13**, L785 (2001).
[46] R. Jin, J. He, S. McCall, C. S. Alexander, F. Drymiotis, and D. Mandrus, Phys. Rev. B **64**, 180503 (2001).
[47] Z. Hiroi, T. Yamauchi, T. Yamada, M. Hanawa, Y. Ohishi, O. Shimomura, M. Abliz, M. Hedo, and Y. Uwatoko, J. Phys. Soc. Jpn. **71**, 1553 (2002).
[48] Z. Hiroi and M. Hanawa, J. Phys. Chem. Solids **63**, 1021 (2002).
[49] J. P. Castellan, B. D. Gaulin, J. van Duijn, M. J. Lewis, M. D. Lumsden, R. Jin, J. He, S. E. Nagler, and D. Mandrus, Phys. Rev. B **66**, 134528 (2002).
[50] J.-I. Yamaura and Z. Hiroi, J. Phys. Soc. Jpn. **71**, 2598 (2002).
[51] M. T. Weller, R. W. Hughes, J. Rooke, C. S. Knee, and J. Reading, Dalton Trans. 3032 (2004).

[52] K. Tsuda, M. Oishi, M. Tanaka, M. Hanawa, and Z. Hiroi, in *Proceedings of the Annual Meeting of the Abstracts of the Physical Society of Japan* (The Physical Society of Japan, Tokyo, 2002), p. 562.
[53] C. A. Kendziora, I. A. Sergienko, R. Jin, J. He, V. Keppens, B. C. Sales, and D. Mandrus, Phys. Rev. Lett. **95**, 125503 (2005).
[54] J. C. Petersen, M. D. Caswell, J. S. Dodge, I. A. Sergienko, J. He, R. Jin, and D. Mandrus, Nat. Phys. **2**, 605 (2006).
[55] Y. Matsubayashi, D. Hirai, M. Tokunaga, and Z. Hiroi, J. Phys. Soc. Jpn. **87**, 104604 (2018).
[56] J. Harter, Z. Zhao, J.-Q. Yan, D. Mandrus, and D. Hsieh, Science **356**, 295 (2017).
[57] J. W. Harter, D. M. Kennes, H. Chu, A. de la Torre, Z. Y. Zhao, J.-Q. Yan, D. G. Mandrus, A. J. Millis, and D. Hsieh, Phys. Rev. Lett. **120**, 047601 (2018).
[58] F. Razavi, Y. Rohanizadegan, M. Hajialamdari, M. Reedyk, R. Kremer, and B. Mitrović, Can. J. Phys. **93**, 1646 (2015).
[59] The analysis is straightforwardly applicable to another symmetry like T_{2u} suggested in Refs. [56,57]. See the Supplemental Material [60].
[60] See Supplemental Material at http://link.aps.org/supplemental/10.1103/PhysRevLett.122.147602, which includes Refs. [61,62], for the notations of multipoles, the description of electron hoppings, the microscopic expressions of electric toroidal quadrupoles, and the odd-parity multipoles with T_{2u} symmetry.
[61] J. M. Blatt and V. F. Weisskopf, *Theoretical Nuclear Physics* (Dover Publications, New York, 1991).
[62] H. Kusunose, J. Phys. Soc. Jpn. **77**, 064710 (2008).
[63] S. Hayami and H. Kusunose, J. Phys. Soc. Jpn. **87**, 033709 (2018).
[64] O. Vyaselev, K. Arai, K. Kobayashi, J. Yamazaki, K. Kodama, M. Takigawa, M. Hanawa, and Z. Hiroi, Phys. Rev. Lett. **89**, 017001 (2002).
[65] S. Hayami, M. Yatsushiro, Y. Yanagi, and H. Kusunose, Phys. Rev. B **98**, 165110 (2018).
[66] D. J. Singh, P. Blaha, K. Schwarz, and J. O. Sofo, Phys. Rev. B **65**, 155109 (2002).
[67] H. Harima, J. Phys. Chem. Solids **63**, 1035 (2002).
[68] Note that the imaginary hoppings correspond to the MT dipoles on the bond centers. In fact, the BO state in Fig. 2(a) has a net MT dipole moment.
[69] S. Raghu, X.-L. Qi, C. Honerkamp, and S.-C. Zhang, Phys. Rev. Lett. **100**, 156401 (2008).
[70] M. Kurita, Y. Yamaji, and M. Imada, J. Phys. Soc. Jpn. **80**, 044708 (2011).
[71] T. Goto, Y. Nemoto, K. Sakai, T. Yamaguchi, M. Akatsu, T. Yanagisawa, H. Hazama, K. Onuki, H. Sugawara, and H. Sato, Phys. Rev. B **69**, 180511 (2004).
[72] S. Kasahara, H. Shi, K. Hashimoto, S. Tonegawa, Y. Mizukami, T. Shibauchi, K. Sugimoto, T. Fukuda, T. Terashima, A. H. Nevidomskyy *et al.*, Nature (London) **486**, 382 (2012).
[73] M. Yoshizawa, D. Kimura, T. Chiba, S. Simayi, Y. Nakanishi, K. Kihou, C.-H. Lee, A. Iyo, H. Eisaki, M. Nakajima *et al.*, J. Phys. Soc. Jpn. **81**, 024604 (2012).
[74] T. Asaba, B. J. Lawson, C. Tinsman, L. Chen, P. Corbae, G. Li, Y. Qiu, Y. S. Hor, L. Fu, and L. Li, Phys. Rev. X **7**, 011009 (2017).
[75] H. Watanabe and Y. Yanase, Phys. Rev. B **98**, 245129 (2018).
[76] Y. Matsubayashi, K. Sugii, H. T. Hirose, D. Hirai, S. Sugiura, T. Terashima, S. Uji, and Z. Hiroi, J. Phys. Soc. Jpn. **87**, 053702 (2018).
[77] J. S. Gardner, M. J. P. Gingras, and J. E. Greedan, Rev. Mod. Phys. **82**, 53 (2010).